Midbody assembly and its regulation during cytokinesis

Chi-Kuo Hu[a,b], Margaret Coughlin[a], and Timothy J. Mitchison[a]
[a]Department of Systems Biology and [b]Graduate Program in Biological and Biomedical Sciences, Harvard Medical School, Boston, MA 02115

ABSTRACT The midbody is a transient structure that connects two daughter cells at the end of cytokinesis, with the principal function being to localize the site of abscission, which physically separates two daughter cells. Despite its importance, understanding of midbody assembly and its regulation is still limited. Here we describe how the structural composition of the midbody changes during progression throughout cytokinesis and explore the functional implications of these changes. Deriving from midzones, midbodies are organized by a set of microtubule interacting proteins that colocalize to a zone of microtubule overlap in the center. We found that these proteins split into three subgroups that relocalize to different parts of the midbody: the bulge, the dark zone, and the flanking zone. We characterized these relocalizations and defined domain requirements for three key proteins: MKLP1, KIF4, and PRC1. Two cortical proteins—anillin and RhoA—localized to presumptive abscission sites in mature midbodies, where they may regulate the endosomal sorting complex required for transport machinery. Finally, we characterized the role of Plk1, a key regulator of cytokinesis, in midbody assembly. Our findings represent the most detailed description of midbody assembly and maturation to date and may help elucidate how abscission sites are positioned and regulated.

INTRODUCTION

After the furrow ingression in cytokinesis, dividing animal cells are partitioned into two daughters but remain connected for some time by a narrow intracellular bridge known as the midbody. Since its initial description by Walther Flemming in the 19th century (Flemming, 1891), the midbody has drawn sporadic attention from cytologists (Buck and Tisdale, 1962; Mullins and Biesele, 1977; Mullins and McIntosh, 1982; Euteneue and McIntosh, 1980; Saxton and McIntosh, 1987). These descriptions revealed a tightly packed, antiparallel microtubule bundle at its core, embedded in a matrix of material that stains darkly by electron microscopy (EM), whose

composition is unknown. Mass spectrometry assays showed that midbodies contain proteins not only related to the cytoskeleton, but also involved in other pathways, such as lipid rafts and vesicle trafficking (Skop et al., 2004). A complex composition is not surprising, given that the midbody coordinates cytoskeletal processes with abscission, which is membrane based. The midbody in animal cells is considered to share certain similarities with the cell plate in plant cell division (Flemming, 1891; Paweletz, 2001). Some, although not all, microtubules in the cell plate are interdigitated, overlapping, antiparallel microtubules covered with electron-dense material accumulations (Hepler and Jackson, 1968; Austin et al., 2005; Ho et al., 2011) and are required for completing the last step of cell division. A challenge in analyzing midzones has been the presence of a region at the center that excludes antibodies, making immunofluorescence problematic (Mullins and McIntosh, 1982; Saxton and McIntosh, 1987; Dhonukshe et al., 2006). Thus, despite having a list of midbody proteins, our knowledge of precisely how they are organized and targeted to midbodies is limited.

The midbody forms from the midzone—a bipolar microtubule array that assembles between separating sister chromatids during anaphase (also called the central spindle; Figure 1A). Conversion of midzones to midbodies correlates positively with furrow ingression.
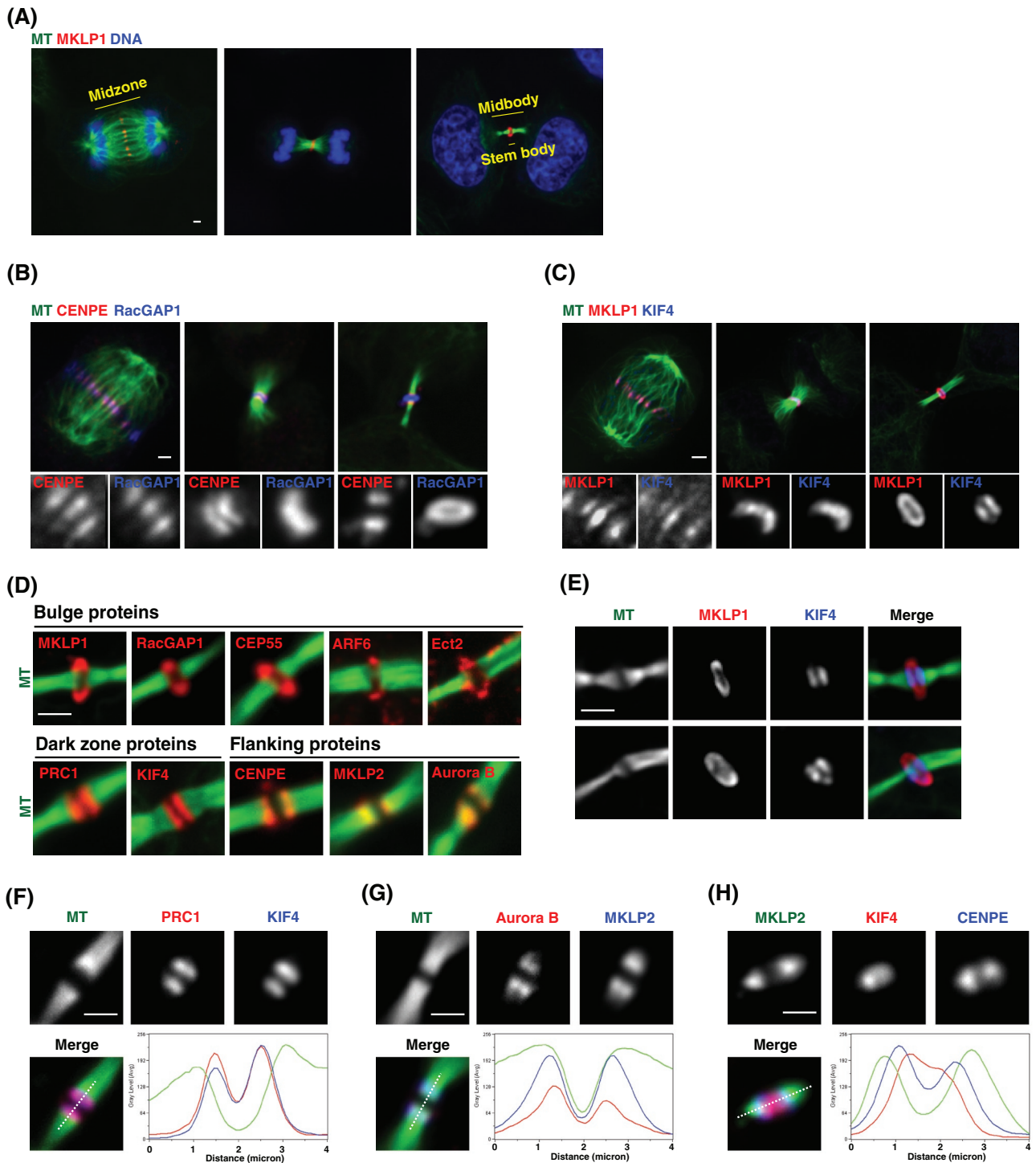
FIGURE 1: Midzone proteins show distinct relocalization patterns during midbody formation. Cells in different stages of cytokinesis were fixed for immunofluorescence. (A) Midzones between separated sister chromatids gradually converted into the midbody during furrow ingression. Individual midzone bundles were compacted into a single, large, midbody microtubule bundle. A bulge-like structure named the stem body was formed in the center of midbody. The midzone, midbody, and stem body are indicated in yellow. (B) CENPE colocalized with RacGAP1 on midzones in anaphase but relocalized to flank RacGAP1 after furrow ingression onset. (C) MKLP1 and KIF4 colocalized on midzones in anaphase and during furrow ingression but changed to different localizations after furrow ingression. (D) Midbody proteins were categorized into three groups according to their localizations on the midbody in immunofluorescence. All localizations were concluded with observations from a minimal sample size of 50 cells in which >97% showed the same localization patterns. (E) MKLP1 on the bulge localized exclusively to KIF4 on microtubules. (F–H) Localizations of proteins on midbody microtubules were determined and compared by line scans. Peaks of line scans were used as references. PRC1 and KIF4 peaked at the same positions where microtubule signal was low. Aurora B and MKLP2 peaked at the same positions where microtubule signal was high. Line scans of three different kinesins MKLP2, CENPE, and KIF4 peaked at different positions. Bar, 3 μm.

Blocking furrow ingression causes cells to accumulate with midzone-like microtubule assemblies (Straight *et al.*, 2003). The furrow is believed to compact antiparallel midzone bundles into the single large bundle that comprises the core of the midbody. During compaction, a bulge that develops at the center of midbody is called the stem body (Figure 1A). The electron-dense material that initially forms on the center of midzone bundles accumulates in this bulge, and accommodating it may generate the bulged shape (Buck and Tisdale, 1962; Euteneuer and McIntosh, 1980). Midzone assembly is somewhat understood. The core circuitry involves two kinesins (centralspindlin and KIF4) collaborating with an antiparallel cross-linker (PRC1) to organize and stabilize a narrow zone of plus-end overlap at the center of the midzone in a process regulated by two kinases (Aurora B and Plk1; Glotzer, 2009). All these proteins and their interaction partners colocalize to microtubule bundles in a narrow plane at the center of midzones. Some authors assumed that they remain colocalized during the conversion of midzones to midbodies, but in fact they split into differentially localized subgroups, as we will show. We suspect that these subgroups have different functions in midbodies.

The main function of the midbody is presumably to localize abscission. Recently, significant progress has been made on molecular mechanisms of both abscission and midbody breakage that precedes it. Abscission may be driven by the endosomal sorting complex required for transport (ESCRT) machinery and midbody breakage by activity of microtubule-severing proteins (Gromley *et al.*, 2005; Morita *et al.*, 2007; Lee *et al.*, 2008; Elia *et al.*, 2011; Guizetti *et al.*, 2011). However, how the ESCRT machinery and severing proteins are localized and temporally regulated is unknown. One problem for analyzing the role of different proteins in midbody assembly and abscission is that most known midbody proteins are also required for furrow ingression, and so knocking them down causes earlier defects that preclude analysis of their specific roles on the midbody later. We became interested in this problem from analysis of monopolar cytokinesis, in which early cytokinesis events are relatively normal but midbody formation is not and usually fails (Canman *et al.*, 2003; Hu *et al.*, 2008). Here we provide the first detailed description of how known midbody proteins localize during late steps in cytokinesis. We then investigate how these assembly events are regulated and their functional implications.

RESULTS

Midzone proteins relocalize during midbody formation

A similar set of proteins localize to both midzones and midbodies (Doxsey, 2005; Gromley *et al.*, 2005), but precisely how their localizations change has not been described. We observed that midbody proteins began changing their localizations during the furrow ingression. Relative timing was evaluated in fixed cells, in which we staged progress through cytokinesis by the extent of furrow ingression and by characteristic midbody morphology, as described previously (Hu *et al.*, 2011). These relocalization events were not necessarily occurring simultaneously. For example, CENPE, KIF4, and centralspindlin (MKLP1 and RacGAP1) colocalized on midzones in anaphase (Figure 1, B and C). CENPE started to differ in localization from the other proteins during furrow ingression (Figure 1B). KIF4, however, remained colocalized with centralspindlin until the completion of furrow ingression and then relocalized (Figure 1C). In each case, while centralspindlin remained at the center and appeared as a single ring in some images, the protein other than centralspindlin moved to a more exterior location. Thus different midzone proteins relocalize in different spatiotemporal patterns during its maturation into the midbody.

We extended this analysis to a set of proteins with conserved roles in cytokinesis that localize to midzones and midbodies. By immunofluorescence, midbody proteins could be categorized into three groups (Figure 1D). The bulge at the center of the midbody accumulated centralspindlin and its known interaction partners CEP55, ARF6, and Ect2 (Boman *et al.*, 1999; Yuce *et al.*, 2005; Zhao *et al.*, 2006; Hutterer *et al.*, 2009). A narrow region on the microtubule bundle in the center of the midbody, where tubulin staining is blocked, accumulated the known interacting pair PRC1 and KIF4. We refer to this localization as the "dark zone" in reference to its antibody-excluding characteristic. Dark-zone proteins appeared as two closely spaced bands by immunofluorescence, but we suspect that they also extend between the two bands, since they form a single band by expression of green fluorescent protein (GFP)–tagged proteins (Zhu and Jiang, 2005; Hu *et al.*, 2011). Two broader bands on microtubules outside the dark zone accumulated CENPE, MKLP2, and Aurora B. We will refer to this region as the flanking zones. We suspect flanking-zone proteins are not continuous throughout the midzone, since they also appear as split bands by GFP expression (Murata-Hori and Wang, 2002; Elia *et al.*, 2011).

Proteins in the bulge (MKLP1) and in the dark zone (KIF4) were mutually exclusive in localization (Figure 1E). Protein localizations on microtubules were determined by line scans along the midbody microtubule bundles. KIF4 and PRC1 shared the same immunofluorescence localizations in the dark zone (Figure 1F). However, proteins flanking the dark zone did not always colocalize. For example, although kinesin MKLP2 and its cargo Aurora B (Gruneberg *et al.*, 2004) showed a close colocalization on microtubules flanking the dark zone (Figure 1G), another kinesin, CENPE, appeared to localize closer to the dark zone with a smaller flanking gap than MKLP2. Costaining of three kinesins MKLP2, CENPE, and KIF4 showed layered localizations on microtubules, with KIF4 in the dark zone, CENPE flanking the dark zone, and MKLP2 on the outsides (Figure 1H). This was not an artifact from chromatic aberration in microscopy, since switching labeling dyes did not change the order of layered localizations (unpublished data). Our data showed that, including MKLP1 on the bulge and KIF4, CENPE, MKLP2 on microtubules, at least four kinesins localized at different parts of the midbody, suggesting a complex structure of the midbody.

Midbody protein localizations in the stem body

Thin-section EM was used to examine the detailed structure of the midbody. Traditional horizontal sections showed enriched electron-dense materials in the stem body at the center and compressed microtubules at the presumptive abscission sites (Figure 2A), which were also called narrow constriction sites (Mullins and Biesele, 1977; Elia *et al.*, 2011). Serial cross sections at the stem body showed that both the bulge and the space between microtubules were filled by electron-dense materials (compare Figure 2B, b′ and c′, blue arrows in insets). Vesicles were observed to accumulate beside but not within the stem body (Figure 2B, b′, red arrows). We conclude that the stem body is a highly compact structure that is filled with electron-dense material and may physically exclude vesicles.

It has long been documented that some proteins in the stem body cannot be revealed by immunofluorescence, presumably because antibody penetration in this area is blocked by the high density of microtubules, associated proteins, and electron-dense materials (Mullins and McIntosh, 1982; Saxton and McIntosh, 1987). An alternative that has not been ruled out is local chemical modifications of epitopes, but this would have to affect many different proteins at once. Owing to this epitope-masking feature, protein localizations in the stem body have not been well documented and are
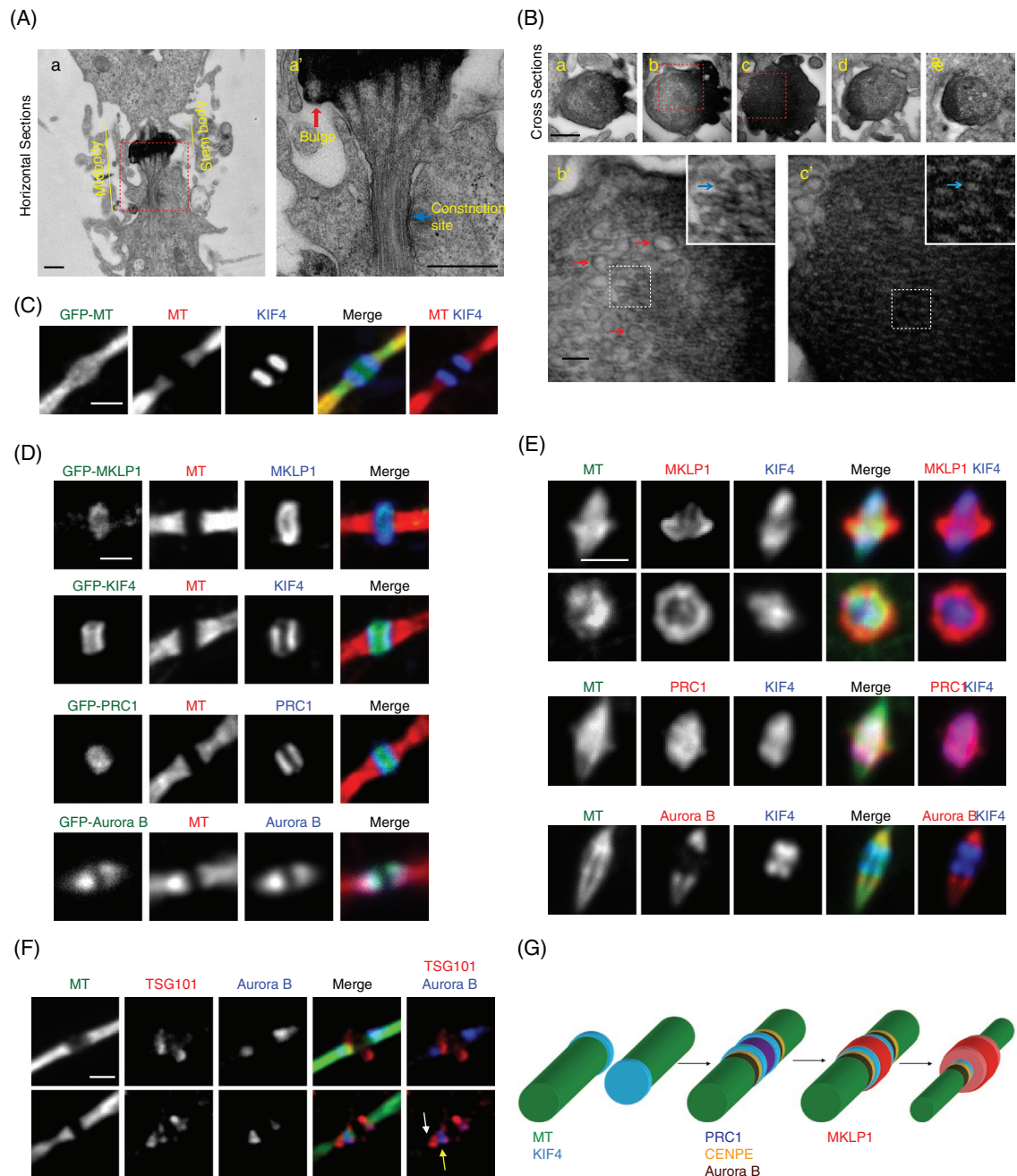
FIGURE 2: Structure and protein localizations in the dark zone of stem body. (A) Thin-section EM of the midbody. Electron-dense material was enriched in the stem body, and microtubules were compressed at presumptive abscission sites. The area boxed in red was magnified and shown on the right (a′). The midbody and stem body are indicated by yellow lines and the bulge and presumptive abscission site by red and blue arrows, respectively. (B) Series cross-section EM of the stem body. Areas boxed in red (b, c) were magnified (b′, c′). Microtubules within or besides the stem body are boxed in white and magnified (insets in b′ and c′). Vesicles accumulated besides, but not within, the stem body. Vesicles and microtubules are indicated by red and blue arrows, respectively. Electron-dense material was observed to fill the space between microtubules within, but not besides, the stem body. (C) Cells with preabscission or postabscission midbodies were fixed for immunofluorescence. GFP-tubulin (GFP-MT) was observed in the dark zone. KIF4 staining was observed in outer regions of the dark zone. Tubulin staining was masked throughout the whole dark zone. (D) GFP fusion proteins were expressed at low level to reveal their localizations in the dark zone. GFP-MKLP1 localized on the bulge, GFP-KIF4 localized in the dark zone as two bands, and GFP-PRC1 filled the dark zone. GFP-Aurora B was excluded from the stem body. (E) Immunofluorescence of endogenous proteins on midbody remnants. Tubulin staining was continuous in midbody remnant. MKLP1 localized on the bulge as a ring by horizontal views, not on microtubules in the stem body. KIF4 localized as two distinct bands, and PRC1 filled the stem body. Aurora B was excluded from KIF4 localizations on midbody remnants. (F) Cells with midbodies at early (top) and late (bottom) stages of cytokinesis were fixed for immunofluorescence. TSG101 was first concentrated on the bulge and both sides of the stem body and then appeared on the presumptive abscission sites (white arrow) after narrowing onset, exclusive to Aurora B (yellow arrow). (G) Proposed model of midbody structure and formation. Bar, 500 nm (A–B), 100 nM (B, b′–c′), 3 μm (C–E).

usually assumed to be the same. We observed that the masking effect was not identical in the whole dark zone. Whereas all immunofluorescence was masked in the inner core of dark zone, only tubulin staining was blocked in the outer regions of the stem body, and proteins on the bulge were not masked at all (Figures 1E and 2C). We tried different cell fixation methods using formaldehyde, methanol, or trichloroacetic acid. However, none of them could unmask the immunofluorescent dark zone of the stem body (unpublished data).

To reveal protein localizations in the dark zone, we transfected cells with GFP-tagged midbody proteins. However, overexpressed GFP-MKLP1, GFP-KIF4, and GFP-PRC1 saturated the stem body and lost specificity in their localizations (Supplemental Figure S1A). To overcome this obstacle, we expressed GFP fusion proteins at low levels to avoid saturating the stem body. GFP-MKLP1 was observed in the bulge only. GFP-KIF4 and GFP-PRC1, which shared identical immunofluorescence localizations, actually localized differently in the dark zone. GFP-KIF4 appeared as two distinct bands, whereas GFP-PRC1 filled the whole dark zone (Figure 2D).

We also found, unexpectedly, that the stem body was no longer masked in immunofluorescence after abscission, evidenced by the continuous tubulin staining on midbody remnants (Figure 2E). Immunofluorescences of endogenous MKLP1, KIF4, PRC1, and Aurora B on midbody remnants were consistent with results of low-level expressed GFP fusion proteins. A horizontal view of midbody remnants further confirmed that MKLP1 was absent from microtubules and localized on the bulge as a ring (Figure 2E). This important kinesin seems to relocalize from a microtubule-bound state in midzones to an unbound but trapped state in the bulge in midbodies. Aurora B was observed to localize at both ends of midbody remnants, next to abscission sites (Figure 2E). Immunofluorescence of preabscission midbodies confirmed that the cortical contraction of abscission always occurred near the border of Aurora B localizations (Supplemental Figure S1B). Aurora B kinase activity inhibits abscission (Steigemann et al., 2009). The spatial correlation between abscission site and the outer border of Aurora B localization in the flanking zone suggests that Aurora B might negatively regulate abscission-site positioning in the stem body and thus help localize abscission to the outer edges of the midbody. It has been shown that membrane trafficking regulators, such as soluble N-ethylmaleimide–sensitive factor attachment protein receptor (SNAREs), Exocyst, and ESCRTs, are recruited to the midbody as part of the abscission machinery (Gromley et al., 2005; Morita et al., 2007; Lee et al., 2008; Elia et al., 2011; Guizetti et al., 2011). We thus costained ESCRT protein TSG101 with Aurora B and MKLP1 (Figure 2F and Supplemental Figure S1C). Consistent with previous studies (Elia et al., 2011), TSG101 was observed to localize on the bulge and both sides of the stem body. However, when the cortical contraction started at the presumptive abscission sites, TSG101 was relocalized at the abscission sites (Figure 2F, white arrow) and was exclusive to Aurora B in localizations (Figure 2F, yellow arrow). To further monitor membrane trafficking to the midbody, we incubated GFP-EB3 expressing HeLa cells with Alexa Fluor 594–conjugated transferrin (Alexa594–transferrin; Supplemental Figure S1D and Movie S1). Growing microtubules indicated by GFP-EB3 were not able to pass the stem body, forming a GFP-EB3–free zone. Alexa594-transferrin–positive endosomes moved along microtubules and then stopped when signals of Alexa594 reached the GFP-EB3–free region (Supplemental Figure S1D, yellow arrows). Later it started to accumulate at the midbody presumptive abscission sites after the onset of cortical contraction (Supplemental Figure S1D, white arrows). Thus trafficking vesicles accumulated at both stem body and narrowed presumptive abscission sites at different stages of the midbody.

Depletion of CEP55 was reported to disturb the midbody formation and also to unmask the immunofluorescent dark zone of the stem body (Zhao et al., 2006). However, our results showed that CEP55 depletion did not affect epitope masking of the stem body. MKLP1 also localized on the bulge of the stem body normally in the absence of CEP55 (Supplemental Figure S2). These results suggest that midbody formation was not abolished by CEP55 depletion. CEP55 is thus not required for midbody formation but more likely is involved in the later midbody abscission (Lee et al., 2008; Bastos and Barr, 2010).

On the basis of our results and published data, we propose a model of midbody structure shown in Figure 2F. KIF4 localizes to plus ends to terminate microtubule dynamics (Hu et al., 2011). The midbody inherits plus end–terminated antiparallel microtubule bundles from midzones. KIF4 on these interdigitated plus ends thus appears as two distinct bands. PRC1 bundles overlap microtubules between two KIF4 bands and localizes to the dark zone where the overlap is, as expected. MKLP1 apparently dissociates from microtubules to accumulate as the midbody bulge. CENPE and Aurora B then localize on microtubules flanking the stem body in layers.

Domain requirements for stem body protein recruitment

Protein recruitment into the stem body appeared to be a highly selective process. We next explored how these complex arrangements are generated and the nature of their functions. Different protein fragments were used to probe possible principles of this selectivity and arrangement. We focused on localization requirements for three key stem body proteins—MKLP1, KIF4, and PRC1. Localization of GFP-tagged deletion constructs was scored as shown in Figure 3. To summarize these data:

MKLP1: The motor-less C-terminal region of MKLP1 is sufficient for accumulation in the bulge. This is consistent with our suggestion from the cytology that MKLP1 in the bulge is not in direct contact with microtubules. What MKLP1 interacts with to accumulate at this site is an interesting future question.

KIF4: The motor domain is required to focus KIF4 in the stem body. The majority of the motor-less KIF4 fragment accumulated in the nucleus. Only a small subset of it localized as two bands on the stem body.

PRC1: This protein binds and cross-links microtubules through coiled-coil domains in its C-terminal half. Deleting its microtubule binding domain did not abolish PRC1's stem body recruitment but changed its localization from microtubules to the bulge. The N-terminal half of PRC1 forms a complex with KIF4 and MKLP1 but not microtubules (Kurasawa et al., 2004). Similarly, the N-terminal PRC1 fragment was recruited to the stem body but mislocalized to the bulge, where MKLP1 localizes.

A surprising conclusion from this domain analysis is that all three stem body proteins can localize to some extent to the stem body when lacking their microtubule-interacting regions. For the motor-less KIF4, given that the majority was unable to be recruited into the stem body but instead localized in the nucleus, its stem body localization might occur by dimerization with full-length protein since motor-less KIF4 remains at where endogenous KIF4 is in the stem body. For MKLP1 and PRC1, given that their microtubule-binding fragments bound microtubules in the midbody but were excluded from the stem body, this suggests that microtubule-binding ability is not a determinant for stem body recruitment of MKLP1 and PRC1. Instead, their protein–protein interacting domains should play more critical roles in their stem body
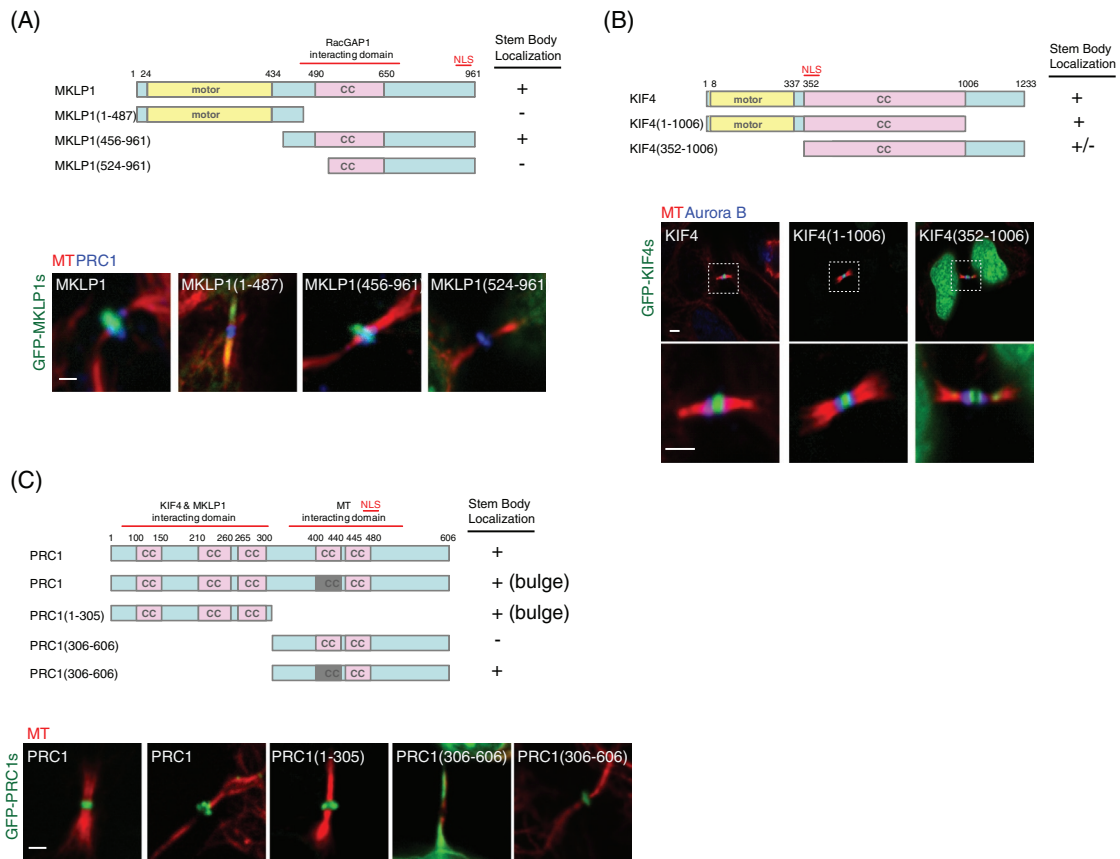
FIGURE 3: Domain mapping of the stem body protein recruitment. Cells expressing GFP-tagged, full-length or truncated MKLP1, KIF4, and PRC1 were fixed for immunofluorescence. Constructs and domain maps are shown as cartoons, with immunofluorescence below. CC, coiled-coil domain; NLS, nuclear localization signal. (A) MKLP1 C-terminal fragment, which contains a complete coiled-coil domain, was recruited to the stem body. MKLP1 N-terminal fragment contains a motor domain localized on microtubules but was excluded from the stem body. (B) Boxed regions are magnified below. KIF4 missing the C-terminal domain was recruited to the stem body. KIF4 missing the motor domain was recruited to the nucleus, with a small portion localized on the stem body as two distinct bands. (C) PRC1 fragment without the C-terminal microtubule-binding domain could still be recruited to the stem body but was on the bulge. PRC1 missing the N-terminal KIF4- and MKLP1-interacting domain localized on microtubules but was excluded from the stem body. Bar, 3 μm.

recruitments. For example, MKLP1 interacting with RacGAP1 to form the centralspindlin complex might be required to recognize the antiparallel microtubule structure of the stem body (Pavicic-Kaltenbrunner et al., 2007; Hutterer et al., 2009). For PRC1 this is probably not the case because deletion constructs lacking microtubule binding fully localized to the bulge, not the microtubule bundle. where endogenous PRC1 is. This suggests that PRC1 might be recruited to the stem body through specific interactions with other stem body proteins. How any protein accumulates in the bulge is unclear.

Protein localization to presumptive abscission sites

After the midbody forms, the cortex starts to contract at both sides of the midbody as two narrow constriction sites that are believed to mature into one or two abscission sites later (Mullins and Biesele, 1977). Proteins that are believed to drive abscission, including SNAREs, ESCRTs, and spastin, are recruited to these sites after midbody assembly (Gromley et al., 2005; Morita et al., 2007; Lee et al., 2008; Elia et al., 2011; Guizetti et al., 2011). How abscission sites are positioned is unknown. None of the microtubule-interacting proteins described in Figure 1 specifically localized in presumptive ab-

scission sites. However, two proteins characteristic of the furrow cortex did localize to these sites. The actin-, myosin-, and septin-binding protein anillin localized not only to the furrow cortex and the midbody bulge as previously reported (Field and Alberts, 1995; Straight et al., 2005; Gregory et al., 2008; Hickson and O'Farrell, 2008), but also to the two presumptive abscission sites just outside the flanking zone (Figure 4A, yellow arrows). Anillin localized to the outer border of Aurora B at these sites (Supplemental Figure S3). The master furrow regulator RhoA also localized to both the midbody bulge and two presumptive abscission sites, indistinguishable from anillin (Figure 4B, yellow arrows). However, not all furrow proteins showed the same localizations on the midbody as anillin and RhoA. Septin (visualized with an antibody to septin7), although not especially enriched, was present at presumptive abscission sites but not the bulge (Figure 4C, yellow arrows). In contrast, citron kinase was only at the bulge but not at the presumptive abscission sites (Figure 4D, blue arrow). These observations suggest the possibility that anillin and RhoA spatially regulate the abscission by affecting ESCRT localizations. Unfortunately, this hypothesis could not be tested by knockdowns because these proteins are required earlier in cytokinesis.
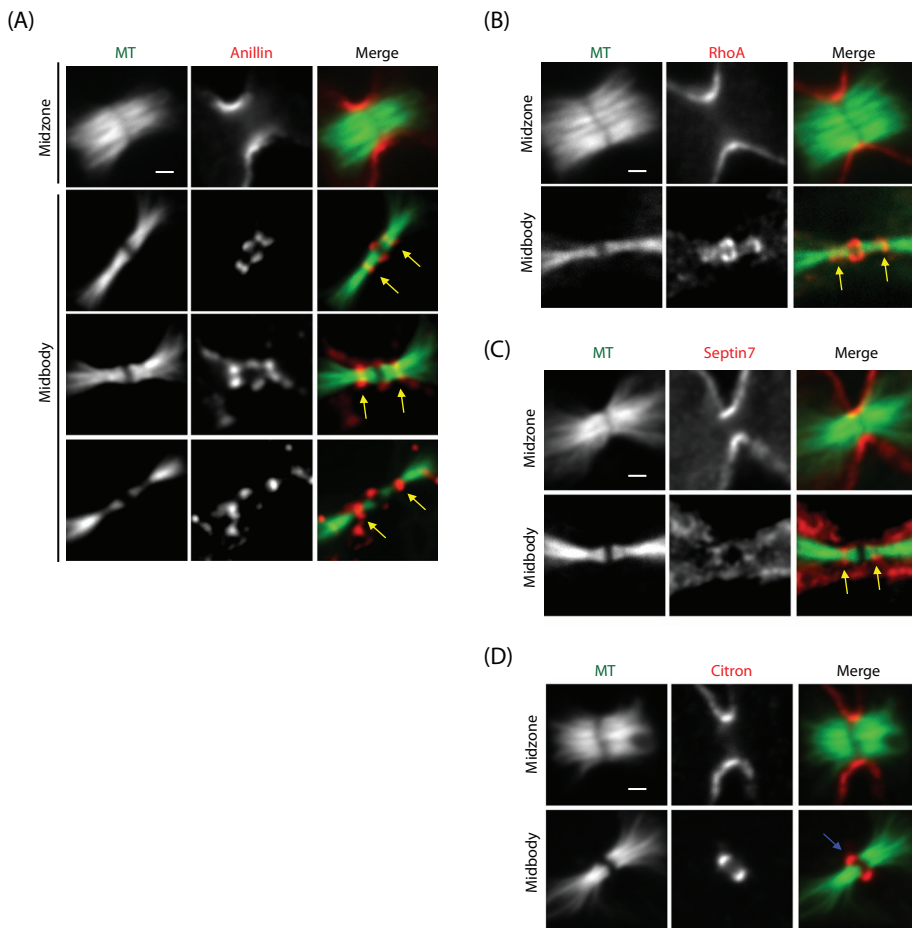
(A)

MT Anillin Merge

Midzone

Midbody

(B)

MT RhoA Merge

Midzone

Midbody

(C)

MT Septin7 Merge

Midzone

Midbody

(D)

MT Citron Merge

Midzone

Midbody

FIGURE 4: Cortical furrow protein localized on the presumptive abscission sites of the midbody. (A) Furrow protein anillin localized on both bulge and presumptive abscission sites (yellow arrows) of the midbody after furrow ingression completed. This localization was observed in 185 of 200 cytokinetic cells (92.5%). (B) Sharing the same furrow localization with anillin, RhoA also localized on both bulge and presumptive abscission sites of the midbody. (C) Septin (septin 7) was observed on the cortical furrow and two presumptive abscission sites (yellow arrows) but not on the bulge. (D) Citron kinase was observed on the bulge (blue arrow) but was absent from presumptive abscission sites of the midbody. Bar, 3 µm.

Furrow ingression is required for midbody formation in cytokinesis

The conversion from midzones to the midbody was initiated after the onset of furrow ingression. Proteins of three categorized groups in Figure 1 initially colocalized on midzones but gradually differed in localizations during this conversion to the midbody. To test whether furrow ingression is required for this process, we treated cells with the small molecule myosin II inhibitor blebbistatin. Previous work showed that this treatment causes cells to accumulate with midzone-like microtubule assembles (Straight *et al.*, 2003), but whether these undergo any kind of maturation in terms of protein localization was not tested. Without furrow ingression, midzone microtubules stayed as individual microtubule bundles, and proteins of three distinct groups in Figure 1 (MKLP1, PRC1, KIF4, and Aurora B) remained colocalized at the center of these microtubule bundles (Figure 5). Latrunculin B, which inhibits actin assembly and furrow ingression, also blocked this protein relocalization characteristic of midbody formation (unpublished data). Thus furrow ingression is required for maturation of midzones into midbodies, including characteristic relocalization of microtubule-binding proteins, as well as compaction.

Plk1 kinase activity is required for midbody formation and maintenance

During the midbody formation, midzone proteins on microtubules changed their localizations to be either recruited to or excluded from the stem body (Figure 1). We noticed that Plk1 uniquely showed both patterns at different stages of cytokinesis (Figure 6A). Plk1 colocalized with stem body marker KIF4 on midzones but was gradually separated from KIF4 during furrow ingression. Then Plk1 relocalized again to enter the stem body late in cytokinesis, after furrow ingression. We observed that in the midbody remnant, which is not masked in immunofluorescence, Plk1 localized continuously throughout the stem body. Both MKLP2 and PRC1 were proposed to transport Plk1 on microtubules during cytokinesis (Gruneberg *et al.*, 2004; Neef *et al.*, 2007). Our results showed that Plk1 initially shared similar localizations with midbody-flanking proteins during furrow ingression and then with dark-zone proteins after furrow completion. These suggest that MKLP2 and PRC1 might both serve as Plk1 carriers but at different time points during cytokinesis. However, due to the preabscission epitope masking of the stem body, we did not exclude the possibility that Plk1 only colocalized with PRC1 after abscission.

We next tested whether Plk1 activity plays any essential role in the stem body formation. Plk1 has multiple functions in different phases of cell division. Thus unsynchronized cells were treated with Plk1 small-molecule inhibitor BI-2536 for only 20 min to avoid carrying early-stage defects to the midbody. In the presence of BI-2536, the stem body did not form (Figure 6B), and no antibody-excluding dark zone was observed by immunofluorescence. Aurora B, PRC1, KIF4, and MKLP1 failed to relocalize to distinct parts of the midbody and stayed colocalized with microtubules, being less focused than in untreated cells. It is intriguing that their localizations were always biased toward one of the daughter cells. Time lapse of GFP-EB3 stably–expressing cells showed that the Plk1 activity was required to maintain the midbody (Figure 6C and Supplemental Movies S1 and S2). The midbody assembled normally in the control. Growing microtubules were blocked by the stem body, forming a GFP-EB3–free zone. In the presence of BI-2536, the preformed midbody disassembled with time, evidenced by gradual encroachment of GFP-EB3 comets into the midbody region. About 30 min after drug addition, presumptive abscission sites widened, and GFP-EB3 comets were able to grow throughout the intracellular bridge. Our data suggest that Plk1 is spatiotemporally regulated in a complex manner, with its kinase activity required to form and maintain the midbody and stem body during cytokinesis.

DISCUSSION

The midbody forms from midzone microtubules that are compressed by the ingressing furrow. Here we characterize a

(A)

Magnified

MT | MKLP1 | PRC1 | Merge | MKLP1 PRC1

Control

Blebbistatin

(B)

Magnified

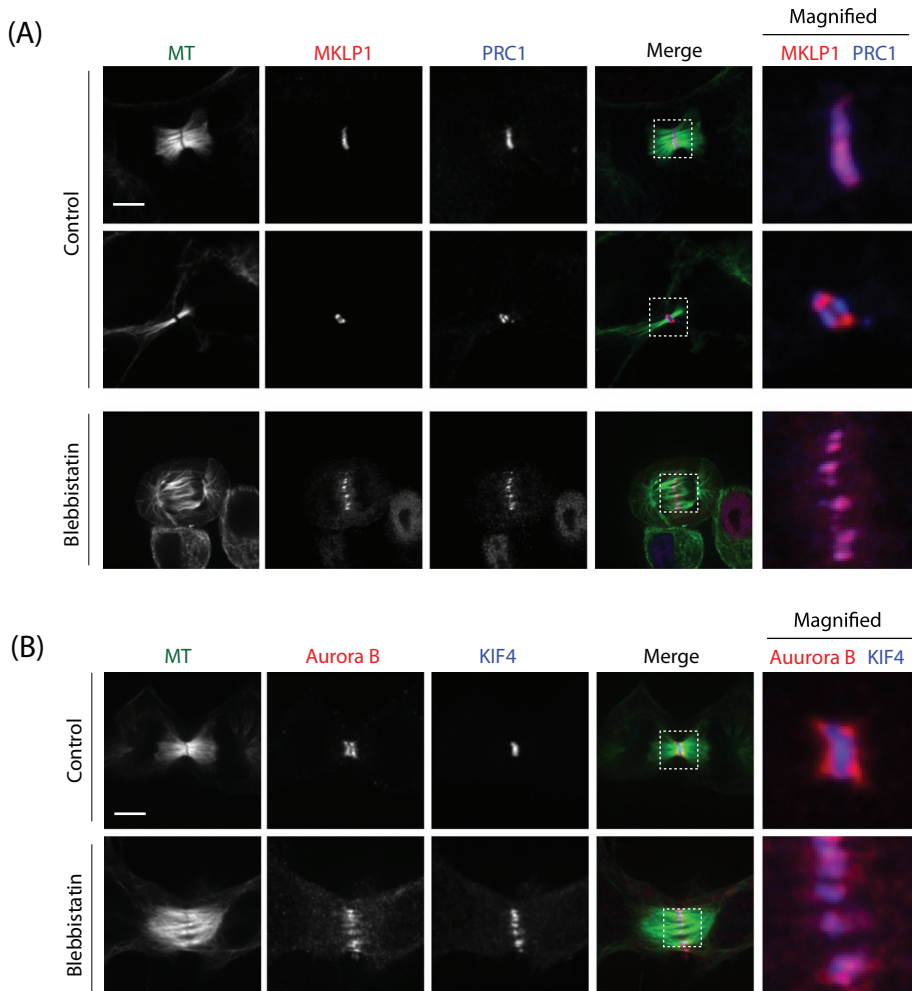MT | Aurora B | KIF4 | Merge | Auurora B KIF4

Control

Blebbistatin

FIGURE 5: Furrow ingression is required for midbody formation. (A, B) Cells were treated with blebbistatin for 30 min and then fixed for immunofluorescence. Furrow ingression was blocked by blebbistatin. Midbody proteins MKLP1, KIF4, PRC1, and Aurora B were still colocalized on microtubules and did not relocalize to distinct parts of the midbody as in control.

complicated relocalization pattern of microtubule-interacting proteins from the center of the midzone to distinct locations in the midbody that accompanies the midbody maturation. This relocalization defines probably biochemically distinct regions in the midbody with different functions—the central bulge, central dark zone, and peripheral flanking regions. The central bulge contains centralspindlin and interacting proteins and appears as a ring by light microscopy (Figure 2, D and E). The bulge contains no or very few microtubules (Figure 2, C and E) and may be the site to which the ingressing furrow finally anchors (Figure 4). A puzzle we did not solve is why some microtubule-interacting proteins, such as centralspindlin, dissociate from microtubules during midbody maturation yet remain highly localized in the bulge. It is not clear whether they are trapped there by a physical barrier or are cross-linked to some solid structure. The function of the bulge is also obscure. Because it stains strongly with RhoA and anillin (Figure 4, A and B), it might serve as a signaling center to organize cortical events in late cytokinesis. The central dark zone is the region where antiparallel microtubules overlap. We believe its function is to provide architectural definition to the midzone. PRC1 localizes there, where it presumably stabilizes the overlap. KIF4 also localizes there, where it serves to inhibit plus-end elongation (Hu et al., 2011). The flanking zones are characterized by Aurora B binding, as well as

several other microtubule-interacting proteins (Figures 1 and 2). We believe the function of this region is to position abscission sites. Abscission occurs at the outer edge of the Aurora B–binding region, consistent with negative regulation by this kinase. An important finding is that RhoA and anillin—two proteins that define the specialized cortex of the furrow—localize to presumptive abscission sites. One or both may function to regulate the ESCRT machinery to these sites, which would provide the first molecular clue to this process.

The midbody selectively recruited certain proteins into the stem body. It appears that the stem body also retains these localizations. For example, after saturation of its endogenous localizations in the stem body, overexpressed KIF4 then exclusively accumulated between two bands in the stem body but not outside two bands on microtubules (Supplemental Figure S1A). This may not be simply due to the antiparallel microtubule structure of the stem body, since KIF4 is capable localizing on nonantiparallel microtubules in monopolar cytokinesis (Hu et al., 2011). Similarly, overexpressed Aurora B was still excluded from the stem body (Figure 2D) but was capable of localizing on antiparallel microtubules if stem body formation was blocked (Figure 6B). Growing microtubules were also unable to enter the stem body (Figure 6C). Previous studies showed that GFP protein alone in cytoplasm is able to diffuse through the intracellular bridge to the other daughter cell (Steigemann et al., 2009). However, photobleaching assays showed that GFP-Aurora B on midbody microtubules is unable to relocalize to the other side of the stem body (Murata-Hori and Wang, 2002). Our data and previous studies (Gromley et al., 2005; Goss and Toomre, 2008; Montagnac et al., 2008) all showed that vesicles accumulate beside, but not within, the stem body. These suggest that the stem body, as such a dense structure, not only might restrict protein localizations, but also might function as a barrier on microtubules between daughter cells.

One of the enduring mysteries in cytokinesis research is the molecular nature of the darkly staining material seen by thin-section EM (Figure 2, A and B). Among our tested proteins, centralspindlin (MKLP1) matched the localizations of this material most closely. Before furrow ingression onset, this material and MKLP1 both focus on midzone plus ends in monopolar and bipolar cytokinesis (Hu et al., 2008). After furrow ingression completes, both are observed in the bulge (Figure 6C). However, our and previous EM cross sections (Euteneuer and McIntosh, 1980) both showed that the electron-dense material is also abundant between microtubules in the stem body, where MKLP1 was not found by either immunofluorescence of midbody remnant or GFP-tagged protein expression. This suggests the electron-dense material is not identical to centralspindlin or any of our other tested candidates. Because no single protein we studied colocalized with the darkly staining material, we suspect that it
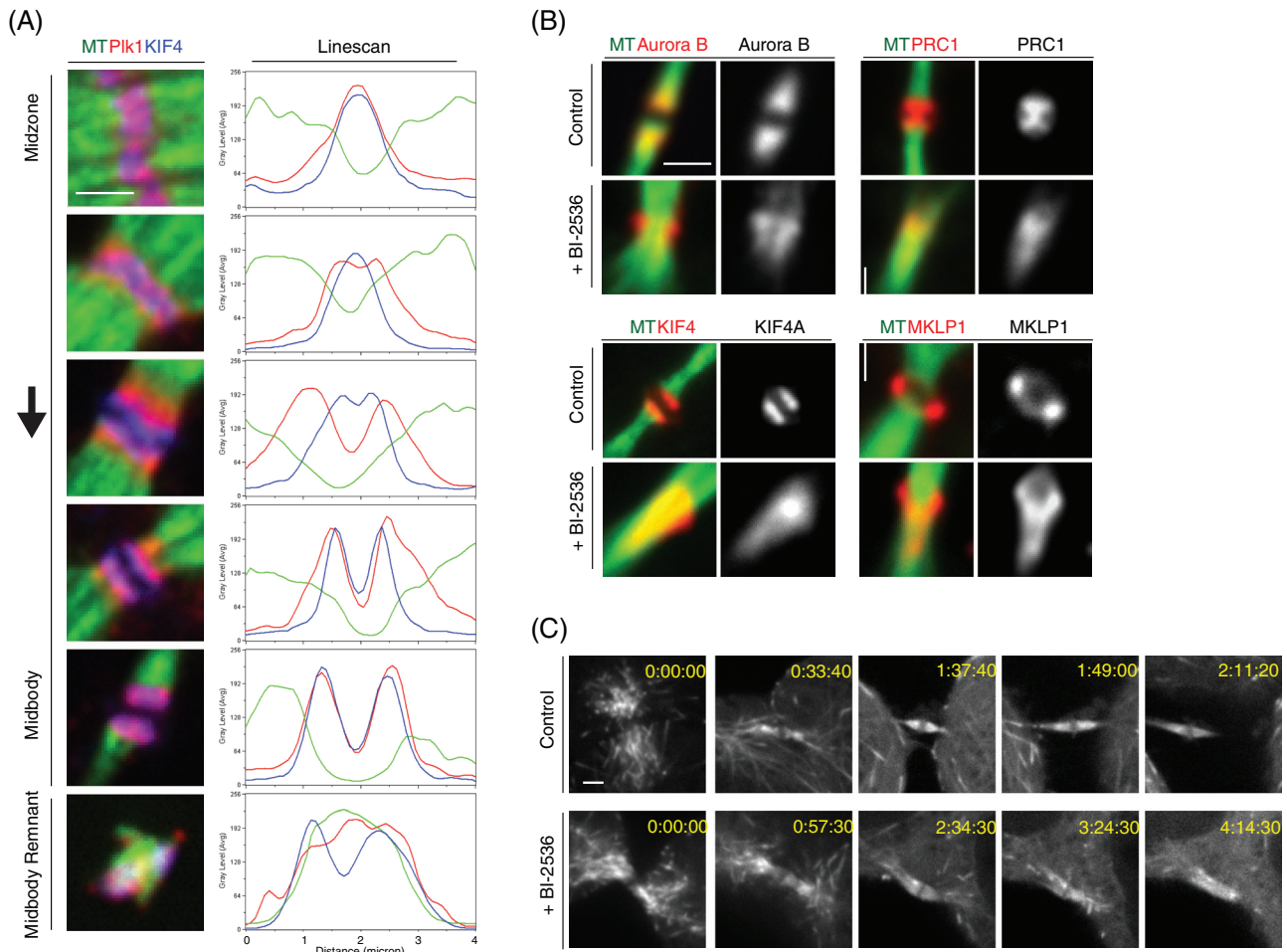
FIGURE 6: Plk1 kinase is required for midbody formation. (A) Cells at different stages of cytokinesis were fixed for immunofluorescence. KIF4 was used as a stem body marker. Line scans were used to measure the relative localizations of KIF4 and Plk1. Plk1 colocalized with KIF4 on midzones and then relocalized to KIF4-flanking regions. After furrow ingression completed, Plk1 relocalized again into the stem body. Plk1 was observed to localize in the core of stem body on midbody remnant. (B) Cells were treated with BI-2536 for 20 min and then fixed for immunofluorescence. In the presence of BI-2536, no immunofluorescence masking was observed on midbodies. Midbody proteins Aurora B, PRC1, KIF4, and MKLP1 all stayed on microtubules, with their localizations biased toward one side of the midbody. Stem body did not form. (C) Cells stably expressing GFP-EB3 were treated with BI-2536 for time-lapse spinning disk microscopy (see Supplemental Movies S1 and S2). Imaging started at time zero. In the non–BI-2536–treated control, the midbody formed and was abscised. In BI-2536–treated cells, the preformed midbody disassembled with time. The GFP-EB3–free zone gradually disappeared. GFP-EB3 eventually was able to move through the intracellular bridge. No abscission occurred. Bar, 3 μm.

may also be the consequence of posttranslational modifications that occurs on multiple proteins in the bulge and dark zone. Its appearance by EM suggests some unusual biochemistry that warrants further study.

Midbody assembly and function are regulated by at least three kinases—Cdk1, Aurora B, and Plk1. Cdk1 activity is down-regulated postanaphase to activate cytokinesis related proteins. The roles of Aurora B and Plk1 have been difficult to pinpoint because they have so many functions throughout cell division. Plk1 showed a unique and dynamic localization in midbodies and midzones. Inhibiting its kinase activity blocked midbody protein relocalizations and stem body formation, culminating in breakdown of the midbody and invasion of the intracellular bridge by dynamic microtubules (Figure 6C). Some likely targets of Plk1 that mediate its midzone functions have been identified, although no doubt many others await discovery. CEP55 recruitment on microtubules was negatively regulated

by Plk1 phosphorylation of CEP55 (Bastos and Barr, 2010). MKLP1—the anchor protein of CEP55 on the midbody—was reported to have a functional role in midbody stabilization (Matuliene and Kuriyama, 2004). MKLP1 interacting with PRC1 was negatively regulated by Plk1 phosphorylation on PRC1 Thr602 (unpublished data). Thus Plk1 might spatiotemporally regulate stem body formation by relocalizing to the stem body after furrow ingression, where its kinase activity releases CEP55 and MKLP1 to form the bulge during late cytokinesis.

Much remains to be done to characterize how midbodies assemble and function. Of particular interest is the question of how they recruit and regulate the abscission machinery. Recent identification of the roles of microtubule-severing proteins and ESCRT complexes in abscission has enabled molecular analysis of abscission. Our observation that RhoA and anillin localize to presumptive abscissions sites suggests a role of these proteins in recruiting or

activating the abscission effector complexes. We did not investigate some of the more exotic suggested functions of midzones, which include communication with centrosomes (Piel *et al.*, 2001; Doxsey, 2005; Gromley *et al.*, 2005) and specification of cell fate (Dubreuil *et al.*, 2007). It can be hoped that our cytological descriptions of midzone architecture and dynamics will enable such studies in the future.

MATERIALS AND METHODS
Cell culture and reagents
HeLa cells were cultured in DMEM with 10% fetal bovine serum at 37°C and 5% CO_2. HeLa cells stably expressing GFP–β-tubulin and GFP-EB3 were gifts from Paul Chang (MIT, Cambridge, MA) and James Orth (Harvard Medical School, Boston, MA), respectively. Cells were incubated with 100 nM BI-2536 (N. Gray, Harvard Medical School) to inhibit Plk1 kinase activity. To induce monopolar cytokinesis, HeLa cells were arrested as monopoles by an overnight incubation with 2 µM kinesin-5 inhibitor *S*-trityl-L-cysteine (Merck, Darmstadt, Germany) and then treated with 2 µM Cdk1 inhibitor RO-3306 (Axon MedChem, Groningen, Netherlands) to force cytokinesis onset. For domain-mapping experiments, GFP-fused mouse KIF4 constructs were gifts from Nobutaka Hirokawa (University of Tokyo, Tokyo, Japan), in which GFP is fused to C-terminal mouse KIF4. For other GFP-tagged constructs, GFP was at the N-terminus of fusion proteins. GFP-Aurora B was a gift from Yu-Li Wang (Carnegie Mellon University, Pittsburgh, PA). GFP-MKLP1, GFP-KIF4, and GFP-PRC1 were directly cloned from PCR product to pEGFP vectors. SMARTpool siRNA (Dharmacon, Lafayette, CO) was used for silencing specific genes. Four specific siRNAs for each gene from SMARTpool were mixed in lower concentration to avoid potential off-target effects.

Immunofluorescence
HeLa cells on coverslips were fixed by 3.7% formaldehyde for 15 min at room temperature, pure MeOH for 3 min, or 10% trichloroacetic acid for 15 min on ice and blocked and incubated with primary or secondary antibodies in AbDil buffer for 45 min. Sources of antibodies were as follows: Plk1 and Aurora B, N. Ozlu and C. Field (Harvard Medical School); Ect2, M. Glotzer (University of Chicago, Chicago, IL); and MKLP2, T. Mayer (University of Konstanz, Konstanz, Germany). PRC1 (sc9342, sc8356), MKLP1 (sc867), RhoA (sc179), ARF6 (sc7971), and Plk1 (sc17783) were from Santa Cruz Biotechnology (Santa Cruz, CA); RacGAP1 (ab2270), CENPE (ab5093), KIF4A (ab3815), and TSG101 (ab83) were from Abcam (Cambridge, MA); citron (611376) was from BD Transduction Laboratories (Lexington, KY); CEP55 (H00055165-A01) was from Abnova (Walnut, CA); (fluorescein isothiocyanate–conjugated) monoclonal anti–α-tubulin (DM1A) and Hoechst were from Sigma-Aldrich (St. Louis, MO); and Alexa Fluor 594–labeled transferrin (T13343) and Alexa Fluor 488–, 594–, or 647–labeled donkey anti-mouse, rabbit, or goat antibodies were from Molecular Probes (Invitrogen, Carlsbad, CA).

Fluorescence microscopy and imaging
Fluorescence images were done by Nikon TE-2000 spinning-disk confocal microscope with a 1.3 numerical aperture, 100× oil-immersion objective (Nikon, Melville, NY). Images were captured on the Hamamatsu Photonic OrCA ER charge-coupled device camera (Hamamatsu, Hamamatsu, Japan) for fixed samples or Andor electron-multiplying charge-coupled device camera (Andor, South Windsor, CT) for live imaging. Microscope control and image processing were through MetaMorph software (Universal Imaging, Molecular Devices, Sunnyvale, CA).

Electron microscopy
HeLa cells were grown on Aclar cover slips. They were fixed with 3% glutaraldehyde in 0.05 M cacodylate buffer, pH 7.0, for 20 min, rinsed with buffer, then postfixed with 1% osmium with 0.8% $K_3Fe(CN)_6$ in buffer for 15 min on ice, in hood. They were then rinsed with distilled water and stained overnight with 1% aqueous uranyl acetate. The following morning, they were rinsed in distilled water and dehydrated in a graded ethanol series using progressive lowering of temperature. They were then infiltrated with solutions of propylene oxide/epon araldite at 1:2, 2:1 before 100% epon araldite. Samples were then mounted and polymerized. Once polymerized, telophase cells were identified, excised, and oriented for cross sectioning and reembedded. A Reichert Ultracut S (Reichert, Depew, NY) was used to cut 75-nm serial sections, which were picked up on slot grids. Sections were counterstained and then viewed on a Tecnai G Spirit BioTwin (FEI, Hillsboro, OR) and imaged with an AMT 2k charge-coupled device camera (Advanced Microscopy Techniques, Woburn, MA).

REFERENCES
Austin JR 2nd, Segui-Simarro JM, Staehelin LA (2005). Quantitative analysis of changes in spatial distribution and plus-end geometry of microtubules involved in plant-cell cytokinesis. J Cell Sci 118, 3895–3903.

Bastos RN, Barr FA (2010). Plk1 negatively regulates Cep55 recruitment to the midbody to ensure orderly abscission. J Cell Biol 191, 751–760.

Boman AL, Kuai J, Zhu X, Chen J, Kuriyama R, Kahn RA (1999). Arf proteins bind to mitotic kinesin-like protein 1 (MKLP1) in a GTP-dependent fashion. Cell Motil Cytoskeleton 44, 119–132.

Buck RC, Tisdale JM (1962). The fine structure of the mid-body of the rat erythroblast. J Cell Biol 13, 109–115.

Canman JC, Cameron LA, Maddox PS, Straight A, Tirnauer JS, Mitchison TJ, Fang G, Kapoor TM, Salmon ED (2003). Determining the position of the cell division plane. Nature 424, 1074–1078.

Dhonukshe P, Baluska F, Schlicht M, Hlavacka A, Samaj J, Friml J, Gadella TW Jr (2006). Endocytosis of cell surface material mediates cell plate formation during plant cytokinesis. Dev Cell 10, 137–150.

Doxsey SJ (2005). Molecular links between centrosome and midbody. Mol Cell 20, 170–172.

Dubreuil V, Marzesco AM, Corbeil D, Huttner WB, Wilsch-Brauninger M (2007). Midbody and primary cilium of neural progenitors release extracellular membrane particles enriched in the stem cell marker prominin-1. J Cell Biol 176, 483–495.

Elia N, Sougrat R, Spurlin TA, Hurley JH, Lippincott-Schwartz J (2011). Dynamics of endosomal sorting complex required for transport (ESCRT) machinery during cytokinesis and its role in abscission. Proc Natl Acad Sci USA 108, 4846–4851.

Euteneuer U, McIntosh JR (1980). Polarity of midbody and phragmoplast microtubules. J Cell Biol 87, 509–515.

Field CM, Alberts BM (1995). Anillin, a contractile ring protein that cycles from the nucleus to the cell cortex. J Cell Biol 131, 165–178.

Flemming W (1891). Neue Beiträge zur Kenntnis der Zelle. Arch Mikrosk Anat 37, 685–751.

Glotzer M (2009). The 3Ms of central spindle assembly: microtubules, motors and MAPs. Nat Rev Mol Cell Biol 10, 9–20.

Goss JW, Toomre DK (2008). Both daughter cells traffic and exocytose membrane at the cleavage furrow during mammalian cytokinesis. J Cell Biol 181, 1047–1054.

Gregory SL, Ebrahimi S, Milverton J, Jones WM, Bejsovec A, Saint R (2008). Cell division requires a direct link between microtubule-bound RacGAP and anillin in the contractile ring. Curr Biol 18, 25–29.

Gromley A, Yeaman C, Rosa J, Redick S, Chen CT, Mirabelle S, Guha M, Sillibourne J, Doxsey SJ (2005). Centriolin anchoring of exocyst and SNARE complexes at the midbody is required for secretory-vesicle-mediated abscission. Cell 123, 75–87.

Gruneberg U, Neef R, Honda R, Nigg EA, Barr FA (2004). Relocation of Aurora B from centromeres to the central spindle at the metaphase to anaphase transition requires MKlp2. J Cell Biol 166, 167–172.

Guizetti J, Schermelleh L, Mantler J, Maar S, Poser I, Leonhardt H, Muller-Reichert T, Gerlich DW (2011). Cortical constriction during abscission involves helices of ESCRT-III-dependent filaments. Science 331, 1616–1620.

Hepler PK, Jackson WT (1968). Microtubules and early stages of cell-plate formation in the endosperm of *Haemanthus katherinae* Baker. J Cell Biol 38, 437–446.

Hickson GR, O'Farrell PH (2008). Rho-dependent control of anillin behavior during cytokinesis. J Cell Biol 180, 285–294.

Ho CM, Hotta T, Guo F, Roberson RW, Lee YR, Liu B (2011). Interaction of anti-parallel microtubules in the phragmoplast is mediated by the microtubule-associated protein MAP65–3 in Arabidopsis. Plant Cell 23, 2909–2923.

Hu CK, Coughlin M, Field CM, Mitchison TJ (2008). Cell polarization during monopolar cytokinesis. J Cell Biol 181, 195–202.

Hu CK, Coughlin M, Field CM, Mitchison TJ (2011). KIF4 regulates midzone length during cytokinesis. Curr Biol 21, 815–824.

Hutterer A, Glotzer M, Mishima M (2009). Clustering of centralspindlin is essential for its accumulation to the central spindle and the midbody. Curr Biol 19, 2043–2049.

Kurasawa Y, Earnshaw WC, Mochizuki Y, Dohmae N, Todokoro K (2004). Essential roles of KIF4 and its binding partner PRC1 in organized central spindle midzone formation. EMBO J 23, 3237–3248.

Lee HH, Elia N, Ghirlando R, Lippincott-Schwartz J, Hurley JH (2008). Midbody targeting of the ESCRT machinery by a noncanonical coiled coil in CEP55. Science 322, 576–580.

Matuliene J, Kuriyama R (2004). Role of the midbody matrix in cytokinesis: RNAi and genetic rescue analysis of the mammalian motor protein CHO1. Mol Biol Cell 15, 3083–3094.

Montagnac G, Echard A, Chavrier P (2008). Endocytic traffic in animal cell cytokinesis. Curr Opin Cell Biol 20, 454–461.

Morita E, Sandrin V, Chung HY, Morham SG, Gygi SP, Rodesch CK, Sundquist WI (2007). Human ESCRT and ALIX proteins interact with proteins of the midbody and function in cytokinesis. EMBO J 26, 4215–4227.

Mullins JM, Biesele JJ (1977). Terminal phase of cytokinesis in D-98s cells. J Cell Biol 73, 672–684.

Mullins JM, McIntosh JR (1982). Isolation and initial characterization of the mammalian midbody. J Cell Biol 94, 654–661.

Murata-Hori M, Wang YL (2002). Both midzone and astral microtubules are involved in the delivery of cytokinesis signals: insights from the mobility of aurora B. J Cell Biol 159, 45–53.

Neef R, Gruneberg U, Kopajtich R, Li X, Nigg EA, Sillje H, Barr FA (2007). Choice of Plk1 docking partners during mitosis and cytokinesis is controlled by the activation state of Cdk1. Nat Cell Biol 9, 436–444.

Pavicic-Kaltenbrunner V, Mishima M, Glotzer M (2007). Cooperative assembly of CYK-4/MgcRacGAP and ZEN-4/MKLP1 to form the centralspindlin complex. Mol Biol Cell 18, 4992–5003.

Paweletz N (2001). Walther Flemming: pioneer of mitosis research. Nat Rev Mol Cell Biol 2, 72–75.

Piel M, Nordberg J, Euteneuer U, Bornens M (2001). Centrosome-dependent exit of cytokinesis in animal cells. Science 291, 1550–1553.

Saxton WM, McIntosh JR (1987). Interzone microtubule behavior in late anaphase and telophase spindles. J Cell Biol 105, 875–886.

Skop AR, Liu H, Yates J 3rd, Meyer BJ, Heald R (2004). Dissection of the mammalian midbody proteome reveals conserved cytokinesis mechanisms. Science 305, 61–66.

Steigemann P, Wurzenberger C, Schmitz MH, Held M, Guizetti J, Maar S, Gerlich DW (2009). Aurora B-mediated abscission checkpoint protects against tetraploidization. Cell 136, 473–484.

Straight AF, Cheung A, Limouze J, Chen I, Westwood NJ, Sellers JR, Mitchison TJ (2003). Dissecting temporal and spatial control of cytokinesis with a myosin II Inhibitor. Science 299, 1743–1747.

Straight AF, Field CM, Mitchison TJ (2005). Anillin binds nonmuscle myosin II and regulates the contractile ring. Mol Biol Cell 16, 193–201.

Yuce O, Piekny A, Glotzer M (2005). An ECT2-centralspindlin complex regulates the localization and function of RhoA. J Cell Biol 170, 571–582.

Zhao WM, Seki A, Fang G (2006). Cep55, a microtubule-bundling protein, associates with centralspindlin to control the midbody integrity and cell abscission during cytokinesis. Mol Biol Cell 17, 3881–3896.

Zhu C, Jiang W (2005). Cell cycle-dependent translocation of PRC1 on the spindle by Kif4 is essential for midzone formation and cytokinesis. Proc Natl Acad Sci USA 102, 343–348.